Original citation:
Roman, Claudia, García-Morales, Moisés, Gupta, Jaipal and McNally, Tony. (2017) On the phase affinity of multi-walled carbon nanotubes in PMMA : LDPE immiscible polymer blends. Polymer, 118. pp. 1-11.

Permanent WRAP URL:
http://wrap.warwick.ac.uk/87883

Copyright and reuse:
The Warwick Research Archive Portal (WRAP) makes this work by researchers of the University of Warwick available open access under the following conditions. Copyright © and all moral rights to the version of the paper presented here belong to the individual author(s) and/or other copyright owners. To the extent reasonable and practicable the material made available in WRAP has been checked for eligibility before being made available.

Copies of full items can be used for personal research or study, educational, or not-for-profit purposes without prior permission or charge. Provided that the authors, title and full bibliographic details are credited, a hyperlink and/or URL is given for the original metadata page and the content is not changed in any way.

Publisher's statement:
© 2017, Elsevier. Licensed under the Creative Commons Attribution-NonCommercial-NoDerivatives 4.0 International http://creativecommons.org/licenses/by-nc-nd/4.0/

A note on versions:
The version presented here may differ from the published version or, version of record, if you wish to cite this item you are advised to consult the publisher's version. Please see the 'permanent WRAP URL' above for details on accessing the published version and note that access may require a subscription.

For more information, please contact the WRAP Team at: wrap@warwick.ac.uk

warwick.ac.uk/lib-publications

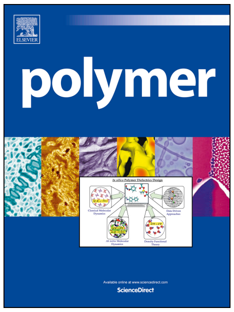

On the phase affinity of multi-walled carbon nanotubes in PMMA:LDPE immiscible polymer blends

Claudia Roman, Moisés García-Morales, Jaipal Gupta, Tony McNally

PII: S0032-3861(17)30428-7

DOI: 10.1016/j.polymer.2017.04.050

Reference: JPOL 19631

To appear in: *Polymer*

Received Date: 22 February 2017

Revised Date: 18 April 2017

Accepted Date: 20 April 2017

Please cite this article as: Roman C, García-Morales Moisé, Gupta J, McNally T, On the phase affinity of multi-walled carbon nanotubes in PMMA:LDPE immiscible polymer blends, *Polymer* (2017), doi: 10.1016/j.polymer.2017.04.050.

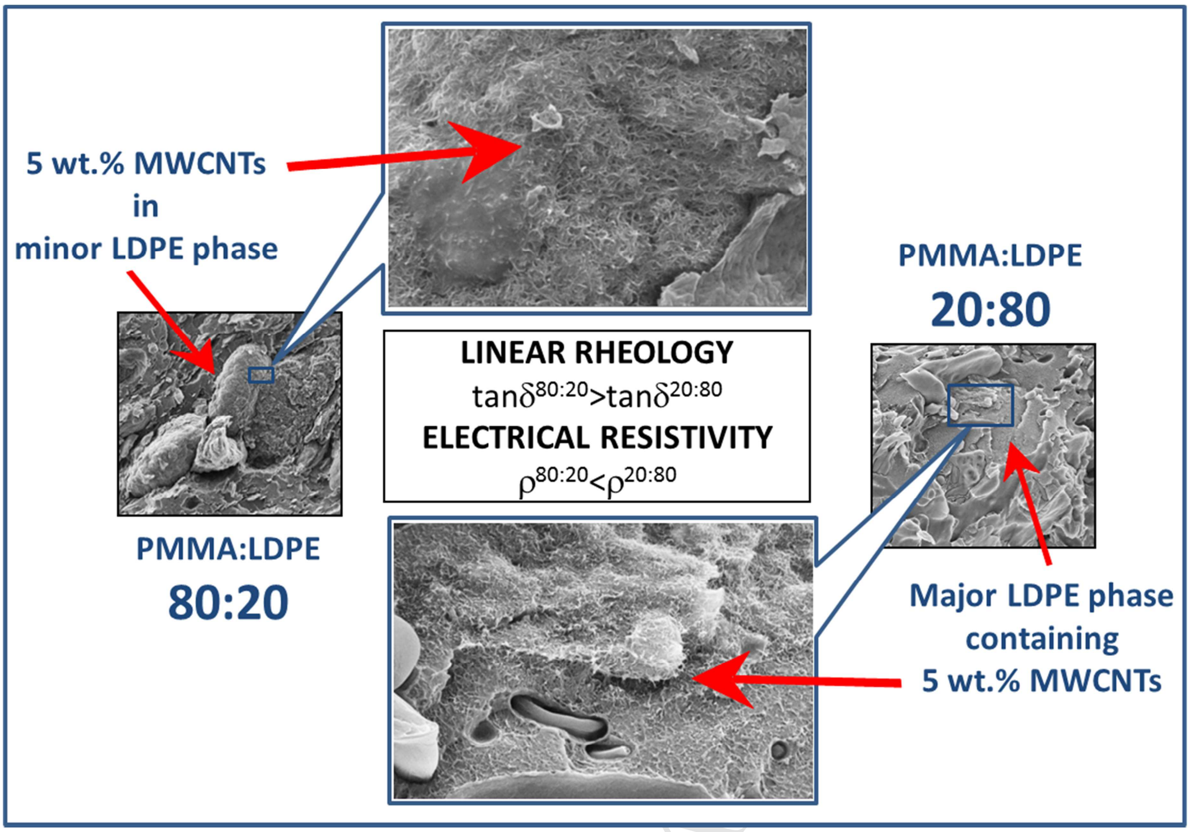
5 wt.% MWCNTs
in
minor LDPE phase
PMMA:LDPE
80:20
LINEAR RHEOLOGY
$\tan\delta^{80:20} > \tan\delta^{20:80}$
ELECTRICAL RESISTIVITY
$\rho^{80:20} < \rho^{20:80}$
PMMA:LDPE
20:80
Major LDPE phase
containing
5 wt.% MWCNTs

On the phase affinity of multi-walled carbon nanotubes in PMMA:LDPE immiscible polymer blends

Claudia Roman[1], Moisés García-Morales[1*], Jaipal Gupta[2] and Tony McNally[2]

[1] *Departamento de Ingeniería Química, Centro de Investigación en Tecnología de Productos y Procesos Químicos (Pro2TecS), Campus de "El Carmen", Universidad de Huelva, 21071, Huelva (SPAIN)*

[2] *International Institute for Nanocomposites Manufacturing (IINM), WMG, University of Warwick, CV4 7AL, (UNITED KINGDOM)*

[*]Author to whom correspondence should be addressed:

Moisés García-Morales, PhD

E-mail: moises.garcia@diq.uhu.es

Phone: +34 959 21 82 07

Fax: +34 959 21 99 83

ABSTRACT

The localization of multi-walled carbon nanotubes (MWCNTs) in PMMA/LDPE blends was studied. Theoretical predictions suggested their preferential localization in the PMMA. Conversely, experimental work revealed that non-functionalized MWCNTs located in the LDPE, polymer first to melt. When the extrusion time is not long enough, the MWCNTs do not have the chance to further migrate to the thermodynamically most favourable phase. The evolution of a double percolation determined if the composite became semi-conductive. In that sense, two blends with PMMA to LDPE ratios of 80:20 and 20:80 containing 2 wt.% MWCNTs had electrical resistivity values in the order of 10^5 and 10^{12} $\Omega \cdot$cm, respectively. Only in the 80:20 blend was the “effective” MWCNT concentration high enough such that electrical percolation was attained. However, bulk rheological properties were controlled by the major phase. Thus, 2 wt.% MWCNTs had a notable effect on the linear viscoelasticity at low frequencies of the 20:80 blend.

Keywords: Poly(methyl methacrylate), Low density polyethylene, Multi-walled carbon nanotubes

1. Introduction

Binary immiscible polymer blends may provide improved performance as compared to their separate constituents, since it is possible to take advantage of specific properties from one or both polymers. Moreover, composites of polymer blends and multi-walled carbon nanotubes (MWCNTs) are of special interest in a number of technological applications [1]. In this regard, their potential performance might be conditioned by the phase where the MWCNTs localize. The thermodynamic wetting parameter, based on the Young equation, has been largely used to successfully predict the selective localization of different filler particles (e.g. MWCNTs, carbon black, carbon fibers and nanoclays) in many immiscible polymer blends. Cardinaud and McNally [2] theoretically predicted and experimentally proved the preferential localization of MWCNTs in the PET phase of several PET/LDPE blends. The same result was achieved by Yesil et al. [3] for PET/HDPE and Goldel et al. [4] found that even minor differences in the wetting behavior were enough for MWCNTs with large aspect ratios to migrate to the more favorable PC phase in PC/SAN blends. Moreover, the wetting coefficient also proved to be successful at predicting the locations of three different silica nanoparticles in LDPE/PEO blends [5].

However, other parameters can govern the preferential localization of fillers. By way of example, Baudouin et al. [6] demonstrated that, in PA12/EA blends, partial irreversible adsorption of the polymer first to wet the MWCNTs (EA) can prevent their complete migration from the interface to the preferred PA12 phase. Zhao et al. [1] also reported that localization is greatly controlled by the mixing protocol employed. That is, when MWCNTs were premixed with PS and further blended with PVDF, more than 30 min. was required for the filler to migrate to the thermodynamically preferred PVDF phase because the viscosity of this polymer at the mixing temperature was much higher than

PS. Moreover, carbon black (CB) was found in the LDPE phase of a PMMA/LDPE blend, even though the wetting coefficient predicted that CB should locate to the PMMA phase for dispersion [7]. The authors again attributed this phenomenon to the higher viscosity of the PMMA phase.

With regard to nanocomposite characterization and properties, the electrical properties of polymer matrices containing CNTs have been the subject of a large number of research papers. Above the so-called electrical percolation threshold, the filler arrangement is such that electrical conductivity is allowed as continuous interconnected filler network is attained. In a binary immiscible polymer blend, the situation becomes much more complex, as the nanoparticles can localize in one phase, in another, in both or even at the interface. The double percolation theory explains that, in case of co-continuous morphology, the electrical percolation limit can be drastically reduced if the filler concentrates in the minor phase or, even better, at the interface [8]. The concept of double percolation, first reported by Sumita et al. [9] for blends filled with CB, provides a theoretical basis for electrical conductivity in immiscible polymer blends. This is turn has led to strategies to reduce the percolation threshold of conductive particles in the final nanocomposite to extremely low values [10,11].

With regard to rheological properties, double percolation does not guarantee a similar effect on the linear viscoelastic properties of the nanocomposite. In contrast to electrical conductivity, rheological percolation in immiscible polymer blends is only achieved if the percolated polymer constitutes the major phase or, at least, significantly contributes to the bulk rheology of the blend. A well-known example of the above mentioned improved performance derived from immiscible polymer blends would be the increased toughness of brittle matrices with rubbers or poly(olefin)s or, inversely, the promotion of enhanced tensile strength in elastomers filled with a brittle polymer [12].

Specifically, several reports have been devoted to blends with varying ratios of poly-(methyl methacrylate) (PMMA) and poly(ethylene)s (LDPE or HDPE). These polymers, which have traditionally been used as commodity plastics, have lately found application in the manufacture of products with high added value [12]. Very few studies have been reported on PMMA/PE blends filled with carbon-based conductive particles (e.g. carbon black, fibers or nanotubes). The published data is mainly composed of morphological characterization based on SEM/TEM observations which the authors use to justify electrical conductivity results based on double percolation theory or to try to reduce the electrical percolation threshold [9,10,13,14]. Moreover, very little attention has been paid to the linear viscoelasticity behaviour of these CNT filled blends. Only Hosseini Pour et al. [7] compared electrical and rheological percolation in a 50:50 PMMA:LDPE blend. However, to the best of our knowledge there has been no case where microscopy analysis and electrical conductivity measurements were used to give further support to a comprehensive rheological characterization, in terms of the effect of polymer ratio and selective CNT localization on the bulk viscoelastic properties. The present article, which explores the localization of MWCNTs in PMMA:LDPE blends, highlights the power of linear rheology as a characterization tool for nano-filled multiphase polymer blends. The results, which demonstrate that rheological percolation is only achieved if the polymer phase having a percolated filler network significantly contributes to the bulk rheology of the blend, were supported and validated by other more frequently used techniques (SEM, DSC and electrical conductivity measurements).

2. Experimental

2.1. Materials

The polymers used in this study were: a) poly(methyl methacrylate) (PMMA) Plexiglas 6N, from Evonik Industries (an amorphous thermoplastic moulding compound, with T_g=99ºC, MVR at 230 ºC/3.8 kg = 12 cm^3/10min, and melt density= 1.10 g/cm^3); b) low density polyethylene (LDPE) LD605BA, from ExxonMobil (a general purpose LDPE grade, with T_m=108 ºC, MFI at 190 ºC/2.16 kg = 6.5 g/10min, and melt density= 0.76 g/cm^3). Non-functionalized multi-walled carbon nanotubes (MWCNTs) NC7000, from Nanocyl S.A, Belgium were used. They are produced via a catalytic carbon vapor deposition (CCVD) process, have average diameter and length of 9.5 nm and 1.5 μm, respectively, and surface area between 250 and 300 m^2/g.

2.2. Composite Blend Preparation

In the first instance, blends of PMMA and LDPE in varying weight proportions of 100:0, 80:20, 60:40, 50:50, 40:60, 20:80 and 0:100 with a constant MWCNT concentration of 2 wt.% were prepared. The formulations for all composite materials prepared are listed in Table 1. Prior to melt mixing both polymers were subjected to cryo-milling, with liquid N_2 in a Freezer/Mill SPEX machine. The fine powder obtained assisted more intimate mixing with the MWCNTs before feeding to the extruder. After milling, all powders were subjected to vacuum drying at 50ºC overnight.

Neat blends (i.e without MWCNTs) were also prepared and used as reference samples. The compounding of all blends was conducted in a co-rotating twin-screw micro-extruder within the interval 180-220 ºC, a Thermo-Haake MiniLab II, at 120 rpm and a mixing time of 5 min. As can be seen from Table 1, the extrusion temperature was progressively decreased with increasing LDPE content, to minimize possible degradation.

In a second set of experiments, two further sets of composites were prepared based on PMMA:LDPE ratios of 80:20 and 20:80, but with varying MWCNT concentration of

0.2, 0.5, 1, 2, 3.5 and 5 wt%. Test specimens were prepared by injection molding using a Thermo-Haake MiniJet II, under 800 bar and for 15 s, see Table 1 for parameters used. Two types of specimens were obtained: a) 25 mm diameter x 1.6 mm thickness disks, for dynamic shear rheology and b) 80 mm x 10 mm x 4 mm bars, for volume electrical resistivity measurements and SEM observations.

2.3. Blend and composite characterisation

The linear viscoelastic properties were evaluated with a controlled-stress rheometer, a Thermo-Haake MARS III equipped with an air convection oven, at a constant temperature of 180 ºC, using smooth plate-plate geometry (25 mm diameter, 1.4 mm gap). The measurement temperature and time were optimized in order to prevent samples from thermal degradation. Firstly, for every sample, dynamic shear stress sweeps, at 1 Hz, were carried out, in order to determine the limit of linear viscoelasticity (LVE). Then, frequency sweep tests were performed between 0.1 and 100 rad/s, at stress values within the LVE regime. At least 3 replicates for each sample were studied.

Differential Scanning Calorimetry (DSC) was conducted on all materials to determine the thermal properties using a Mettler Toledo DSC1 calorimeter with ~10 mg samples placed in aluminium pans, under N_2 gas purge flow. The samples were firstly heated up to 220 ºC and kept for 5 min. in order to erase the thermal history. Then, they were subjected to cooling down to 20 ºC, followed by heating up to 220 ºC, both scans at a rate of 10 K/min.

The volume electrical resistivity of the composite materials was determined using 30 mm x 10 mm x 4 mm bar specimens with a Keithley 6517B-Electrometer, employing a “two-point probe” method [15]. With this approach, two copper strips were glued on the opposite sides of the bar by applying a silver paint. Once dry, a potential difference of 1

V was applied between two electrodes pinched to the copper strips, and the electrical resistance (R) was measured. The volume resistivity was calculated as follows:

$$\rho = \frac{R \cdot S}{l} \qquad (1)$$

where S is the cross-sectional area (0.4 cm^2) and l is the length (3 cm) of the bar specimens. Average values of 3-4 measurements are presented.

The morphology of all composite materials was examined by Field Emission Scanning Electron Microscopy (FE-SEM) at room temperature using a Carl Zeiss Sigma instrument, operating with a 5-10 kV accelerating voltage, at different magnifications. The samples were cryo-fractured using liquid N_2 prior to imaging and the fractured surfaces covered with gold before being exposed to the electron beam.

3. Results and discussion

3.1. Theoretical prediction of phase affinity of MWCNTs

Prior to the experimental being initiated, the localization of MWCNTs in a PMMA/LDPE immiscible polymer blend was theoretically predicted by means of a thermodynamic “wetting coefficient” ω_a [16], which is calculated as follows:

$$\omega_a = \frac{\gamma_{MWCNT-LDPE} - \gamma_{MWCNT-PMMA}}{\gamma_{LDPE-PMMA}} \qquad (2)$$

where $\gamma_{MWCNT-LDPE}$, $\gamma_{MWCNT-PMMA}$ and $\gamma_{LDPE-PMMA}$ are the interfacial energy between MWCNTs-LDPE, MWCNTs-PMMA and PMMA-LDPE, respectively. The lower the interfacial energy between the MWCNTs and polymer, the higher their affinity is. Thus, depending on the value of ω_a obtained, the MWCNTs may localize in either one of the polymer phases or at the interface:

- $\omega_a > 1$, MWCNTs localize preferentially in PMMA.

- $-1 < \omega_a < 1$, MWCNTs localize preferentially at the interface between both polymers.
- $\omega_a < -1$, MWCNTs localize preferentially in LDPE.

In order to estimate the different interfacial tensions needed for the calculation of the wetting coefficients, two different two-component theories are often used. Two-component theories are based on the assumption that the overall surface free energy of a substance (γ) can be calculated as the sum of two contributions, one due to dispersive interactions (γ^d) and one due to polar interactions (γ^p), according to Equation (3):

$$\gamma = \gamma^d + \gamma^p \qquad (3)$$

Firstly, the Fowkes theory is based on a geometric-mean equation, valid between a low energy material and a high energy material, from which the interfacial energy is calculated as follows:

$$\gamma_{1-2} = \gamma_1 + \gamma_2 - 2\cdot\left(\sqrt{\gamma_1^d \cdot \gamma_2^d} + \sqrt{\gamma_1^p \cdot \gamma_2^p}\right) \qquad (4)$$

The second theory, by Wu, is based on a harmonic-mean equation, valid between low energy materials, and is expressed as:

$$\gamma_{1-2} = \gamma_1 + \gamma_2 - 4\cdot\left(\frac{\gamma_1^d \cdot \gamma_2^d}{\gamma_1^d + \gamma_2^d} + \frac{\gamma_1^p \cdot \gamma_2^p}{\gamma_1^p + \gamma_2^p}\right) \qquad (5)$$

In both equations 4 and 5, γ_1 and γ_2 are the surface free energy (surface tensions) of the components 1 and 2, whilst γ_1^d, γ_2^d, γ_1^p, γ_2^p are their dispersive and polar parts, respectively.

For the three components of the composites used in this study (MWCNTs, PMMA and LDPE), the dispersive and polar parts [6,16] and the overall surface free energy, at 20 ºC, are included in Table 2.

However, the wetting coefficient has to be evaluated at the compounding temperature at which the extrusion was conducted. Thus, within the temperature interval at which the different nanocomposites were extruded, an average temperature of 200ºC was used for this calculation. In the case of the polymers, the temperature dependency of the surface free energy can be assumed to be linear at ordinary temperatures such as 0-200 ºC [16], and is expressed by a constant value of (-dγ/dT). For the polymers studied in this work, the corresponding temperature coefficients are shown in Table 3. Moreover, the ratios of the polar and dispersive contributions to the overall surface free energies γ^p/γ and γ^d/γ, respectively, are assumed not to depend on temperature. As for the MWCNTs, their surface free energy is not affected by temperature, i.e. in the temperature range used throughout this study. Therefore, we present in Table 4 the estimated values for the interfacial energy corresponding to the blend component pairs; CNTs-LDPE, CNTs-PMMA and LDPE-PMMA, at 200ºC, based on either the geometric or harmonic models. The resulting values of for wetting coefficients, calculated from Equation (2), are also included. From these values for wetting coefficients (Table 4), it can be concluded that if thermodynamic equilibrium is reached the MWCNTs will preferentially locate within the PMMA phase.

3.2. Experimental evidence for phase affinity

In contrast to the wetting coefficient predictions, the results obtained from different experimental techniques demonstrated that MWCNT localization is not always conditioned by thermodynamic considerations only. In order to explore the localization of unmodified MWCNTs in the PMMA/LDPE blends, a comprehensive characterization of these composites based on rheological and electrical properties, calorimetry and microscopy was completed.

Oscillatory shear frequency sweep tests, at 180ºC, within the linear viscoelastic (LVE) region were performed. Previous dynamic stress sweep tests demonstrated that, independently of composite formulation, a value of stress of 200 Pa was always within the LVE region at 180ºC.

Figure 1A shows the frequency dependency of the elastic (G′) and viscous (G″) moduli, at 180ºC, for selected unfilled PMMA/LDPE blends and both polymers. It can be observed that PMMA shows the typical behavior expected in its molten state. It consists of a rubbery plateau region at the highest frequencies studied, followed by a drop in its elastic and viscous moduli (approaching the viscous flow region) with decreasing frequency. On the contrary, LDPE shows the typical behavior corresponding to low molecular weight polymers free of entangled networks [17]. That is, its linear rheological behavior is characterized by elastic and viscous moduli curves which monotonically decrease as a function of frequency, with a crossover point which delimits the direct (no rubbery plateau) transition to the viscous flow region. With regard to their blends, it is noteworthy that the addition of 20 wt.% (26.57 vol.%) LDPE to the PMMA matrix (referred to as sample 80:20), if compared to pure PMMA, has a minor effect on the viscous modulus, but increased the elastic modulus at the lowest frequency studied (0.1 rad/s). As the LDPE inclusions are less elastic than the PMMA matrix, this enhanced elasticity is actually attributed to shape relaxation of deformed LDPE droplets driven by interfacial tension. This micromechanical (not molecular) relaxation mechanism, with a characteristic time much higher than the terminal relaxation times of the phases, is responsible for the “secondary plateau” which starts to develop at 0.1 rad/s in Figure 1A [18]. At the highest frequencies, the LDPE dispersed phase is easier to deform than the PMMA matrix, yielding slightly reduced elasticity of the blend [19]. As for the sample 20:80 (a LDPE matrix loaded with 20 wt.% or 14.73 vol.% PMMA), increased values of both Gˈ and G˝ are observed in the whole frequency window studied, although the effect is more significant as the terminal region is approached and for the elastic modulus. As the PMMA inclusions are much more elastic than the matrix, the result observed is due most probably to the reinforcing effect provoked by hard PMMA droplets rather than shape relaxation [20]. An intermediate situation is observed for the 50:50 blend (40.86 vol.% PMMA). This blend presents a reduced plateau region, if compared to neat PMMA, and a crossover point which appears at a frequency value between those corresponding to the pure constituents.

In order to facilitate the understanding of the effect of composition on the elastic properties of the blends, Figure 1B illustrates the evolution of the loss tangent (tanδ=G''/G') with frequency, at 180ºC, as a function of the ratio of PMMA to LDPE. At the highest frequencies studied tanδ monotonically increases with LDPE content, as expected from a higher volume fraction of a phase easier to deform. However, the behavior at the lowest frequencies is much more complex and depends on the polymer constituting the minor phase. Thus, blends with LDPE as the minor phase (i.e. the 80:20 and 60:40 blends) present an enhanced elastic response if compared to pure PMMA. As commented above, this behavior responds to the well-known Palierne emulsion model applied to immiscible polymer blends. Similarly, blends with a minor phase of PMMA (i.e. the 40:60 and 20:80 blends) show much lower tanδ values than pure LDPE, as the more elastic PMMA inclusions enhance the elastic contribution associated with the blend.

Figure 1B shows that the elastic response of the blends is very sensitive to morphology changes at low frequencies. For that reason, tanδ at 180ºC and 0.1 rad/s was plotted versus LDPE content (Figure 1C). The curve presents two distinct parts at both sides of a threshold concentration which lies between 50 and 60 wt.% LDPE. At the left side of this transition the major PMMA phase exerts the main influence on the linear rheological response, whilst at the right side an analogous situation occurs for the major LDPE phase. So, at that point phase inversion occurs, which corresponds to a “fully” co-continuous morphology. Moreover, each part shows a minimum which is associated to the onset of “partial” co-continuity. The left border is located between 20 and 40 wt.% LDPE whereas the right border appears to be between 60 and 80 wt.% LDPE. For LDPE concentrations below or above the interval of dual-phase co-continuity the rheological behavior is governed by a droplet-matrix morphology, and the elastic response becomes higher as the interfacial area (dispersed phase) increases. However, the onset of partial co-continuity (at either side) yields a decrease in the interfacial area and so increased values of tanδ. The maximum value of tanδ is associated to the minimum interfacial area between PMMA and LDPE, which corresponds to full co-continuity or, equivalently, phase inversion. The behavior described is more obvious when the LDPE is the minor phase, a situation which can be successfully described by the emulsion model. Similar behavior has been reported elsewhere [21] for an equi-viscous PP/PS blend. Even though the melt-state linear rheology of PMMA/LDPE blends has not been studied in depth before, the limits of co-continuity and phase inversion concentration herein reported match fairly well with the results obtained by selective solvent extraction on PMMA/HDPE blends conducted by Cheng Zhang et al. [14]. The mixing time affects the domain of co-continuity, in such a way that if it is very long the co-continuity range will tend to a single composition [22]. In contrast, for the 5 min. mixing used in this study the interval is very broad.

The SEM micrographs shown in Figure 2 demonstrate that for LDPE concentrations below and above the limits of dual-phase continuity, the blends exhibit a “sea-island” morphology, characterized by discrete particles of LDPE in a PMMA matrix (80:20 blend in Figure 2A) or of PMMA in a LDPE matrix (20:80 blend in Figure 2B). It is interesting to note the rod-like aspect of the LDPE inclusions in the 80:20 blend when compared to the more rounded LDPE particles in the 20:80 blend. This behavior is probably a consequence of the effects of shear and elongational forces caused by the rotating twin screws on a polymer (LDPE) phase of lower viscosity in a blend which was extruded at higher temperature, i.e. the processing temperature for PMMA. However, for the 50:50 blend, SEM image shown in Figure 2C, both polymer phases prove to have comparable contribution on the blend morphology.

In relation to the composites of PMMA:LDPE blends and MWCNTs, Figure 3 evaluates the effect of 2 wt.% MWCNT addition on the linear viscoelastic behavior of selected blends, as compared to their parent matrices. Figure 3A shows the evolution with frequency, at 180ºC, of the linear viscoelastic moduli for the neat components, PMMA and LDPE, before and after 2 wt.% MWCNT addition. With regard to the LDPE, 2 wt.% MWCNT addition yields increased values of G˙ (mainly) and G˝, as well as decreased slopes of the G˙(ω) and G˝(ω) curves at the lowest frequencies studied. However, the prevailing viscous behavior still remains. In contrast, the viscoelastic behavior of PMMA is significantly altered with 2 wt.% MWCNT addition. Thus, apart from increased values of G˙ and G˝, and the plateau region extending from 3.5 (neat PMMA) down to 1 rad/s, the most remarkable result is the extraordinary enhancement in the elastic behavior in the low frequency region. G˙(ω) and G˝(ω) curves become almost coincident, and with approximate slope of 0.5 on a double-log scale; so, G˙(ω) and G˝(ω) ~ $\omega^{0.5}$, which is often assumed as the rheological criterion for the onset of gel formation [23]. Consequently, addition of 2 wt.% MWCNTs in PMMA, the rheological percolation threshold has been attained (or even surpassed). This behavior, characteristic of ‘pseudo-solid-like’ materials, is facilitated by a MWCNT network which constrains the long range motion of PMMA polymer chains [7]. In contrast, a percolated network was not reached for the LDPE with the same MWCNT concentration.

For the pure components, PMMA and LDPE, the theoretical calculations presented above can support an explanation for the behavior observed. There is much lower interfacial energy, at the PMMA extrusion temperatures so CNTs dispersion in PMMA is easier than in LDPE. As a consequence, for a constant loading of 2 wt.% MWCNTs, the pure PMMA undergoes a higher level of modification than the pure LDPE and rheological percolation is reached at lower MWCNT concentration. Moreover, electrical resistivity values later shown in Figure 4A will prove that pure PMMA becomes semi-conductive with addition of 2 wt.% MWCNTs whereas, at such a concentration, LDPE retains its insulating properties. Some researches claim to have found lower electrical percolation threshold for LDPE or HDPE than for PMMA [7,14]. However, in both of these studies compounding was conducted at constant temperatures (190 and 210 ºC, respectively), which is not the case in our study (220 ºC for PMMA and 180 ºC for LDPE). Under a constant extrusion temperature, a much higher viscosity PMMA might hinder MWCNT diffusion which delays percolation to higher MWCNT loading.

Figure 3B compares the effect of MWCNT addition on the 80:20 and 20:80 blends. The 20:80 blend containing 2 wt.% MWCNTs, for which LDPE constitutes the continuous phase, does not differ much from the pure LDPE containing 2 wt.% MWCNTs (Figure 3A). The main difference is in the higher elasticity of the blend, due to the contribution of the dispersed PMMA phase. However, the situation dramatically changes when the 80:20 blend containing 2 wt.% MWCNTs is analyzed. In this case, MWCNT addition moves both G˙ and G˝ upwards, if compared to the unfilled80:20 blend, but has only a minor effect on either the extent of the plateau or the low frequency regions.

Interestingly, this result hints that the PMMA phase is free of MWCNTs; otherwise, both PMMA and the composite of the 80:20 blend with 2 wt.% MWCNTs should show similar rheological behavior. If fact, Figure 3C, which displays the evolution with frequency of tanδ at 180ºC as a function of the sample composition, shows comparable behavior, in terms of relative elasticity, of the 80:20 blend before and after MWCNT loading (red line and circles, respectively). So, this result suggests that the MWCNTs are preferentially located in the polymer which is not the controlling phase, that is, LDPE. Moreover, the pure PMMA with 2 wt.% MWCNTs shows a peak maximum which indicates network formation. For the the 60:40 blend, the LDPE phase (where MWCNTs preferentially localize) have a much more significant contribution than for the 80:20 blend, and tanδ undergoes an important decrease. Above 40 wt.% LDPE, tanδ increases again as the "effective" MWCNT concentration is reduced with increasing LDPE content.

As a consequence, and in contradiction to the above wetting coefficient prediction, the MWCNTs tend to concentrate in the LDPE phase. A similar result was reported by Hosseini et al. [7] for PMMA/LDPE blends with carbon black and Zhang et al. [14] for PMMA/HDPE blends with short carbon fibers. Thus, other parameters other than thermodynamic considerations can influence the selective localization of MWCNTs. Some authors have shown partial irreversible adsorption of the first polymer to come in contact with MWCNTs during melt mixing [6]. Other authors have also pointed out the importance of polymer melt viscosity [2]. In our one-step processing protocol the MWCNTs are concentrated in the polymer first to melt and with the lowest viscosity, that is, LDPE. Again, it should be noted the extrusion mixing place over a short period of time (5 min.) so that the MWCNTs did not have sufficient time to further migrate to their thermodynamically preferential phase [10].

Volume electrical resistivity measurements, at room temperature, were also carried out on the above blend and composite samples, see Figure 4. Figure 4A, which shows the variation in electrical resistivity with PMMA:LDPE ratio reveals that pure PMMA becomes semi-conductive (resistivity on the order of 10^2 $\Omega\cdot$cm) with addition of 2 wt.% MWCNTs. Therefore, at such a concentration, not only rheological but also electrical percolation has been attained. Conversely, LDPE has electrical resistivity on the order of 10^{13} $\Omega\cdot$cm (it is an insulator). In this case, the electrical percolation threshold has not been attained, similarly for rheological percolation as observed from the linear rheology measurements at 180ºC. With decreasing wt.% LDPE, the resistivity remains almost the same (non-conductive) up to a blend ratio of 50:50. For the blend to be conductive, a so-called “double percolation” [8,9] is required. According to Figure 1C, the LDPE phase is continuous in the above composition range. However, the “effective” MWCNT concentration in the LDPE phase is not large enough such that a conductive network is formed and the composite remains insulating. In contrast, for a blend ratio of 60:40 and, above all, 80:20, the “effective” MWCNT concentration in the LDPE phase is sufficient such that some electrical conductivity is possible. Thus, the resistivity drops down to 10^9 and, then, to 10^5 $\Omega\cdot$cm, respectively. From this result, an important observation can be made. If the resistivity is on the order of 10^5 $\Omega\cdot$cm, this means that even for a PMMA:LDPE blend ratio as high as 80:20 the continuity of the LDPE phase has been, at least partially, attained. Electrical conductivity is not possible if the MWCNT-rich phase is dispersed. This conclusion does not agree with our SEM observations based on the images shown in Figure 2A. However, the inclusion of MWCNTs might have shifted the interval of co-continuity to lower LDPE content, as also reported by Zhang et al. [14] for a PMMA/HDPE blend with short carbon fibers. They attributed this result to the effect of the fibers increasing HDPE melt viscosity. In that sense, Omonov et al.

[21] reported that as the viscosity ratio of the minor less viscous phase to the major more viscous phase (in our case, $\eta^*_{LDPE}/\eta^*_{PMMA}$) approaches 1, mixing becomes more effective because the elongated fibril-like structures formed do not break up and retract. Elastic effects are also important, as a more elastic phase has a tendency to encapsulate a less elastic phase during mixing [24]. As we will show later, LDPE becomes highly elastic with increasing MWCNT addition. For the 80:20 blend, if the “effective” concentration in the LDPE phase iss large enough so that its resulting elasticity becomes comparable to PMMA, sea-island morphology no longer remains. Decreased interfacial tension upon MWCNT addition may also contribute to this new morphology [2].

The SEM micrographs obtained for the above samples, see Figure 5, help further explain this behaviour. Full dual-phase co-continuity for the 50:50 composite (Figure 5C) is quite evident. However, even for a LDPE content as low as 20 wt.% some degree of partial continuity can be appreciated (see Figure 5A) for this polymer. So, for this blend, both requirements of “double percolation” can be fulfilled, what explains why the 80:20 composite had an electrical resistivity in the order of 10^5 Ω·cm. As for the 20:80 composite, the contribution of the PMMA phase to the composite morphology seems to be quite more significant when compared to its unfilled counterpart, see Figure 2B.

In order to further support the rheological and microscopic evidence that the MWCNTs preferentially localize in the LDPE phase, DSC measurements were also conducted. No variation in the melting temperature of pure LDPE (of about 108.5ºC) was observed upon 2 wt.% MWCNT addition (heating scans shown in supplementary data). However, on cooling from the melt, differences were observed in DSC thermograms. Before MWCNT addition, see Figure 6A, the pure LDPE crystallization temperature (T_c) was found at about 94ºC, and was almost not affected when blended with PMMA. After

MWCNT loading, see Figure 6B, the bulk crystallization peak became broader, less sharp and is shifted from 94 to 96.3 ºC for pure LDPE, whilst for the 80:20 composite, with a higher “effective” MWCNT concentration in the LDPE phase, the increase is up to 97.5ºC. Unlike other semi-crystalline polymers, the nucleation effect of MWCNTs in LDPE is not significant [2]. However, it allowed Patra et al. [10] to conclude the preferential dispersion of MWCNTs is in the LDPE phase of PMMA/HDPE blends. Furthermore, as can be seen from Figure 6A a second exothermic peak evolve for LDPE at 60ºC, which has been attributed to a thermal relaxation whose origin is not clear [25]. With increasing PMMA to LDPE ratio, the intensity of this peak decreases and a new crystallization peak develops at about 68ºC. So, apart from the bulk crystallization peak at 94 ºC, the formation of mixed phase morphology yields a second smaller peak (68 ºC) due to homogeneous crystallization of small LDPE droplets [21]. If the PMMA content is further increased up to 80 wt.%, the relaxation peak at 60ºC is no longer observed and, instead, a small peak at 47 ºC arises, most probably due to sea-island morphology (Figure 6A). Conversely, none of the above two homogeneous crystallization peaks are found in Figure 6B probably because the formation of small dispersed drops is partially restrained upon 2 wt.% MWCNT addition.

The effect of varying MWCNT loading on blend properties was also investigated, The influence of MWCNT concentration on rheological properties, at 180ºC, of selected composites was studied by means of frequency sweeps in the LVE regime. Measurements were performed on two blends with PMMA to LDPE ratios of 80:20 and 20:80, as a function of MWCNT concentration up to 5 wt.%. Figure 7A shows that, for the 80:20 blend, the Gˈ and G˝ curves are progressively shifted upwards with increasing MWCNT content. The effect seems to be more evident from 3.5 wt.% onwards. However, as the MWCNTs are preferentially located in the minor LDPE phase, the qualitative behavior of tanδ in Figure 7B remains quite unaltered even at the highest MWCNT concentration of 5 wt.%. Thus, the maximum peak which is associated with the formation of a percolated network does not appear, because the contribution of the LDPE phase to the overall rheology is not significant enough given its low volume fraction (26.75 vol.%). This result is also denoted by the van Gurp-Palmen plot in Figure 7C. No restrictions to long range motion are observed at low frequencies, as all the composites show δ curves which monotonically increase (tend to 90º) with decreasing |G*|. In the same way, similar phase angle values appear as the PMMA entangled network plateau is approached (δ tends to a peak minimum) because short range motion is not constrained. However, from Figure 4B it is known that there is electron transfer between nanotubes, probably via tunneling [10], is possible throughout the LDPE phase when the MWCNT loading is 2wt.%. With increasing MWCNT concentration, the network of nanotubes is enhanced (i.e. increased intimate contact between nanotubes), as denoted by a monotonic reduction in the electrical resistivity down to values on the order of 10^2 Ω·cm. This intimate contact of MWCNTs in the LDPE phase is shown, for 5 wt.%, in Figures 9A1 and A2.

Conversely, MWCNT addition, from a concentration of 2 wt.% upwards, has a significant effect on the linear viscoelastic behavior of the 20:80 blend, as proven from the data in Figure 8A. At 80 wt.% LDPE, this polymer controls the blend bulk rheology because it is the major phase. For that reason, G' (also G″) evolve towards an obvious plateau at the low frequency region with increasing MWCNTs concentration. At 2 wt.% MWCNTs the prevailing viscous behavior of the blend still remains. However, from 3.5 wt.% MWCNTs the elasticity enhancement is so important that the elastic modulus, G', surpasses the viscous modulus, G″, and the crossover point between them disappears. At 5 wt.% the gel-like nature of the composite blend is so strong that, in the frequency range considered, G' resembles the equilibrium modulus which characterizes covalently cross-linked polymer networks [26]. The high concentration of MWCNTs in the LDPE phase shown in Figures 9B is responsible for the rheological behavior observed. Even though full rheological percolation is achieved by 3.5 wt.% MWCNT addition, the onset of percolation formation can be observed in Figure 8B as a clear decrease in loss tangent at the lowest frequencies upon 2 wt.% addition. Moreover, the van Gurp-Palmen diagrams shown in Figure 8C also demonstrate the effect of MWCNT addition on the composites relaxation at large times (low frequencies). A significant reduction in the phase angle values is observed with addition of 3.5 and 5 wt.% MWCNT as a consequence of strong interactions between LDPE chains and nanotubes which hinder polymer long range motion. With regard to the electrical properties, according to Figure 4B, the composite material is still an insulator at 2 wt.% MWCNT inclusion. In fact, the electrical percolation rises only when the nanotubes are in contact or sufficiently close to each other (tunneling effect), a factor not necessary to attain rheological percolation [7]. However, a dramatic decrease in the volume resistivity of six orders of magnitude is observed when the MWCNT concentration was increased from 2 to 3.5 wt.%.

4. Conclusions

The localization of un-functionalized MWCNTs in PMMA/LDPE blends was studied. According to thermodynamic considerations, the PMMA is the most favorable phase due to its higher chemical affinity for the nanotubes. In fact, when added to pure PMMA, their better dispersion yielded electrical and rheological percolation at a lower concentration when compared to pure LDPE. However, MWCNT phase affinity is much more complex when dealing with polymer blends. Experimental work demonstrated the preferential localization of the nanotubes in the LDPE phase, which is the polymer first to melt. Upon entering the extruder, the CNTs concentrated in the polymer phase with the lowest viscosity (LDPE) and, then, did not have the chance to migrate to the second polymer phase (PMMA) before exiting the extruder. Regarding electrical properties, the 80:20 blend became semi-conductive with addition of 2 wt.% MWCNTs. The "effective" CNTs concentration in the LDPE phase was large enough so that the electrical percolation threshold was reached. Moreover, the filler addition transformed the LDPE dispersed phase into a partially continuous phase. This double percolation morphology enabled a dramatic decrease in electrical resistivity. In terms of linear viscoelasticity, no 'solid-like' plateau was observed at low frequency because the MWCNTs did not concentrate in the major phase (PMMA) which controls the composite bulk rheology. With increasing MWCNT concentration, the G' and G″ curves moved vertically but their qualitative behavior, in terms of the viscous-elastic properties balance, did not vary significantly. In contrast, the 20:80 blend with 2 wt.% MWCNTs showed enhanced elasticity at low frequency if compared to its unfilled counterpart. At higher MWCNTs contents, the gel-like nature of the composite material was so strong that the prevailing viscous behavior became elastic and the equilibrium plateau which characterizes covalently cross-linked polymer networks appeared. However, at 2 wt.% MWCNTs, the "effective" concentration was not high enough so that the electrical percolation was attained and the material retained its insulating properties. With increasing MWCNTs concentration up to 3.5 wt.%, the electrical resistivity decreased by six orders of magnitude.

5. Acknowledgements

This work was funded by Ministerio de Educación, Cultura y Deporte (Spain), through the Research Mobility Scholarship (PRX15/00252) awarded to Moisés García-Morales and the Erasmus+ Training Studentship awarded to Claudia Roman. The authors acknowledge the financial support provided by both. MGM and CR thank the IINM (WMG), University of Warwick for hosting their research visit and their kind hospitality.

6. References

[1] X. Zhao, J. Zhao, J-P Cao, D. Wang, G-H Hub, F. Chen, Z-M Dang, Effect of the selective localization of carbon nanotubes in polystyrene/poly(vinylidene fluoride) blends on their dielectric, thermal and mechanical properties, Mater. Design 56 (2014) 807–815.

[2] R. Cardinaud, T. McNally, Localization of MWCNTs in PET/LDPE blends, Eur. Polym. J. 49 (2013) 1287–1297.

[3] S. Yesil, O. Koysuren, G. Bayram, Effect of Microfiber Reinforcement on the Morphology, Electrical, and Mechanical Properties of the Polyethylene/Poly(ethylene terephthalate)/Carbon Nanotube Composites, Polym. Eng. Sci. 50(11) (2010) 2093-2105.

[4] A. Goldel, G. Kasaliwal, P. Potschke, Selective Localization and Migration of Multiwalled Carbon Nanotubes in Blends of Polycarbonate and Poly(styrene-acrylonitrile), Macromol. Rapid Commun. 30 (2009) 423–429.

[5] S. Huang, L. Bai, M. Trifkovic, X. Cheng, C.W. Macosko, Controlling the Morphology of Immiscible Cocontinuous Polymer Blends via Silica Nanoparticles Jammed at the Interface, Macromolecules 49 (2016) 3911−3918.

[6] A.C. Baudouin, J. Devaux, C. Bailly, Localization of carbon nanotubes at the interface in blends of polyamide and ethylene–acrylate copolymer, Polymer 51 (2010) 1341–1354.

[7] S.A. Hosseini Pour, B. Pourabbas, M.S. Hosseini, Electrical and rheological properties of PMMA/LDPE blends filled with carbon black, Mater. Chem. Phys. 143 (2014) 830-837.

[8] A. Goldel, A. Marmur, G. R. Kasaliwal, P. Potschke, G. Heinrich, Shape-Dependent Localization of Carbon Nanotubes and Carbon Black in an Immiscible Polymer Blend during Melt Mixing, Macromolecules 44 (2011) 6094–6102.

[9] M. Sumita, K. Sakata, S. Asai, K. Miyasaka, H. Nakagawa, Dispersion of fillers and the electrical conductivity of polymer blends filled with carbon black, Polym. Bull. 25 (1991) 265-271.

[10] R. Patra, S. Suin, D. Mandal, B.B. Khatua, Sequential Mixing as Effective Method in the Reduction of Percolation Threshold of Multiwall Carbon Nanotube in Poly(methyl methacrylate)/High-Density Poly(ethylene)/MWCNT Nanocomposites, J. Appl. Polym. Sci. 131(10) (2014) 40235.

[11] R. Patra, S. Suin, D. Mandal, B.B. Khatua, Reduction of Percolation Threshold of Multiwall Carbon Nanotube (MWCNT) in Polystyrene (PS)/Low-Density Polyethylene (LDPE)/MWCNT Nanocomposites: An Eco-Friendly Approach, Polym. Composites 36(9) (2015) 1574-1583.

[12] C. Harrats, T. Benabdallah, G. Groeninckx, R. Jerome, Stress–Strain Behavior of Low-Density Polyethylene/Poly(methyl methacrylate) Blends with Modulated Interfaces with a Hydrogenated Polybutadieneblock-Poly(methyl methacrylate) Diblock Copolymer, J. Polym. Sci.: Part B: Polymer Physics 43 (2005) 22–34.

[13] M. Sumita, K. Sakata, Y. Hayakawa, S. Asai, K. Miyasaka, M. Tanemura, Double percolation effect on the electrical conductivity of conductive particles filled polymer blends, Colloid. Polym. Sci. 270 (1992) 134139.

[14] C. Zhang, X-S Yi, H. Yui, S. Asai, M. Sumita, Morphology and Electrical Properties of Short Carbon Fiber-Filled Polymer Blends: High-Density Polyethylene/Poly(methyl methacrylate), J. Appl. Polym. Sci. 69 (1998) 1813–1819.

[15] Y. Singh, Electrical resistivity measurements: a review, Int. J. Modern Phys.: Conference Series, 22 (2013) 745–756.

[16] S. Wu, Polymer interface and adhesion, Marcel Dekker Inc.. New York, 1982.

[17] J.D. Ferry. Viscoelastic properties of polymers, third ed., Wiley, New York, 1980.

[18] M. Bousmina, R. Muller, Linear viscoelasticity in the melt of impact PMMA. Influence of concentration and aggregation of dispersed rubber particles, J. Rheol. 37(4) (1993) 663–679.

[19] D. Lesueur, J.F. Gerard, P. Claudy, J.M. Létoffé, D. Martin, J.P. Planche, Polymer modified asphalts as viscoelastic emulsions, J. Rheol. 42 (1998) 1059–1074.

[20] P.J. Carreau, M. Bousmina, A. Ajji, Rheological Properties of Blends: Facts and Challenges, in: K.P. Ghiggino (Ed.), Progress in Pacific Polymer Science 3,

Proceedings of the Third Pacific Polymer Conference, Springer-Verlag, Berlin, 1994.

[21] T.S. Omonov, C. Harrats, P. Moldenaers, G. Groeninckx, Phase continuity detection and phase inversion phenomena in immiscible polypropylene/polystyrene blends with different viscosity ratios, Polymer 48 (2007) 5917-5927.

[22] M. Castro, C. Carrot, F. Prochazka, Experimental and theoretical description of low frequency viscoelastic behaviour in immiscible polymer blends, Polymer 45 (2004) 4095–4104.

[23] M.E. De Rosa, H.Winter, The effect of entanglements on the rheological behavior of polybutadiene critical gels, Rheol. Acta 33 (1994) 220-237.

[24] A.T. Hedegaard, L. Gu, C.W. Macosko, Effect of Extensional Viscosity on Cocontinuity of Immiscible Polymer Blends [Supporting information], J. Rheol. 59 (2016) 1397.

[25] D. Olmos, E. Rodriguez-Gutierrez, J. Gonzalez-Benito, Polymer Structure and Morphology of Low Density Polyethylene Filled With Silica Nanoparticles, Polym. Composites 33(11) (2012) 2009-2021.

[26] S.B. Ross-Murphy, Structure–property relationships in food biopolymer gels and solutions, J. Rheol. 39(6) (1995) 1451–1463.

Tables

Table 1. PMMA/LDPE volume percentages and processing (extrusion, injection and molding) temperatures for every blend ratio studied.

PMMA:LDPE wt. ratio	**100:0**	**80:20**	**60:40**	**50:50**	**40:60**	**20:80**	**0:100**
vol.% PMMA	100	73.43	50.89	40.86	31.54	14.73	0
vol.% LDPE	0	26.57	49.11	59.14	68.46	85.27	100
Extrusion T (ºC)	220	200	195	195	190	185	180
Melt injection T (ºC)	225	205	205	205	195	190	190
Molding T (ºC)	100	90	90	80	75	75	75

Table 2. Surface free energy values and their dispersive and polar components, at 20ºC, for the nanotubes, PMMA and LDPE.

Component	$\gamma^{d,20^{\circ}C}$ **(mN/m)**	$\gamma^{p,20^{\circ}C}$ **(mN/m)**	$\gamma^{20^{\circ}C}$ **(mN/m) Eq. (3)**
MWCNTs	17.6	10.2	27.8
PMMA	29.6	11.5	41.1
LDPE	35.7	0	35.7

Table 3. Temperature coefficients, and surface free energy values and their dispersive and polar components, at 200ºC, for the nanotubes, PMMA and LDPE.

Component	**-dγ/dT (mN/m·K)**	$\gamma^{d,200^{\circ}C}$ **(mN/m)**	$\gamma^{p,200^{\circ}C}$ **(mN/m)**	$\gamma^{200^{\circ}C}$ **(mN/m) Eq. (3)**
MWCNTs	0	17.6	10.2	27.8
PMMA	0.076	19.75	7.67	27.42
LDPE	0.057	25.44	0	25.44

Table 4. Interfacial energy values, at 200ºC, for the pairs MWCNTs-LDPE, MWCNTs-PMMA and LDPE-PMMA, according to Fowkes (Eq. 4) and Wu (Eq. 5) theories, respectively; their resulting wetting coefficients are included.

Pair	$\gamma_{1-2}^{F,200^{\circ}C}$ **(mN/m)**	$\gamma_{1-2}^{W,200^{\circ}C}$ **(mN/m)**
MWCNTs-LDPE	10.92	11.63
MWCNTs-PMMA	0.24	0.48
LDPE-PMMA	8.03	8.39
Wetting coefficients		
ω_a (unitless)	1.33	1.33

Figure captions

Figure 1. Evolution with frequency, at 180ºC, of the linear viscoelastic moduli (A) and loss tangent (B) for unfilled blends, as a function of PMMA:LDPE ratio. Evolution with LDPE wt. percentage, at 180ºC and 0.1 rad/s, of the loss tangent (C).

Figure 2. SEM micrographs corresponding to unfilled blends with selected PMMA:LDPE ratios: 80:20 (A), 20:80 (B) and 50:50 (C).

Figure 3. Evolution with frequency, at 180ºC, of the linear viscoelastic moduli for the pure polymers (A) and the blends 80:20 and 20:20 (B), before and after 2 wt.% MWCNTs addition. Evolution with frequency, at 180ºC, of the loss tangent for 2 wt.% MWCNTs blends, as a function of PMMA:LDPE ratio (C).

Figure 4. Evolution of the volume electrical resistivity, at ambient temperature, with LDPE wt. percentage for 2 wt.% MWCNTs samples (A) and with MWCNTs wt. concentration for 80:20 and 20:80 samples (B).

Figure 5. SEM micrographs corresponding to 2 wt.% MWCNTs blends with selected PMMA:LDPE ratios: 80:20 (A), 20:80 (B) and 50:50 (C).

Figure 6. DSC cooling scans, at 10 K/min. for unfilled blends (A) and 2 wt.% MWCNTs blends (B) as a function of the PMMA:LDPE ratio.

Figure 7. Evolution with frequency, at 180ºC, of the linear viscoelastic moduli (A) and loss tangent (B), and van Gurp-Palmen plot (C), for blends 80:20 as a function of MWCNTs wt. concentration.

Figure 8. Evolution with frequency, at 180ºC, of the linear viscoelastic moduli (A) and loss tangent (B), and van Gurp-Palmen plot (C), for blends 20:80 as a function of MWCNTs wt. concentration.

Figure 9. SEM micrographs corresponding to 5 wt.% MWCNTs blends with selected PMMA:LDPE ratios: 80:20 (A1 and A2), 20:80 (B1 and B2). Highlighted areas in A1 and B1 appear enlarged in A2 and B2, respectively.

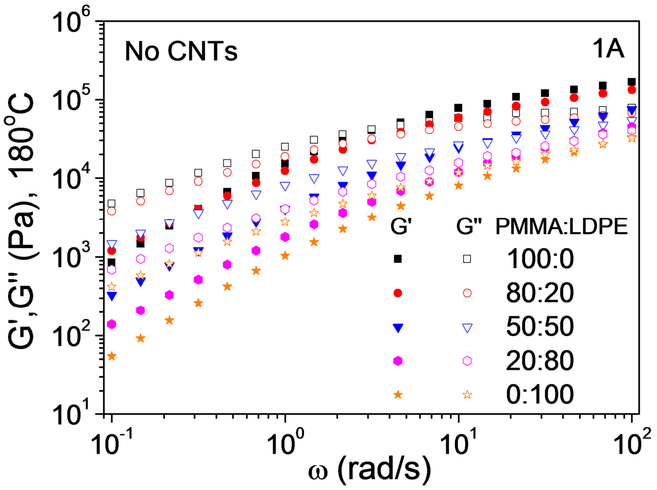
No CNTs
1A
G',G" (Pa), 180°C
ω (rad/s)
10^1
10^2
10^3
10^4
10^5
10^6
10^-1
10^0
10^1
10^2
G'
G"
PMMA:LDPE
100:0
80:20
50:50
20:80
0:100

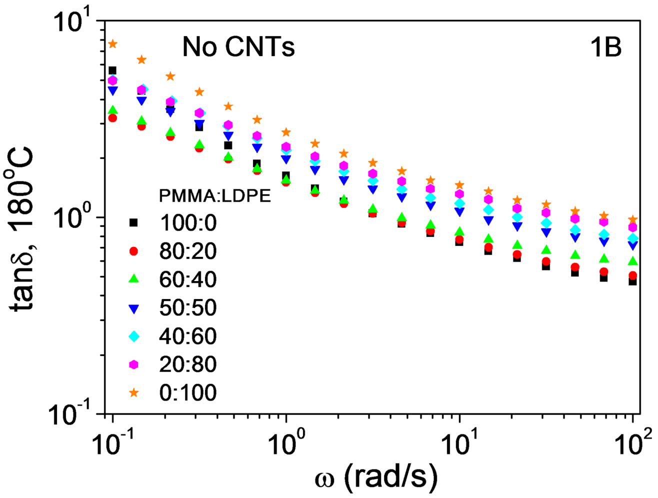
No CNTs
1B
tanδ, 180°C
ω (rad/s)
10^-1
10^0
10^1
10^-1
10^0
10^1
10^2
PMMA:LDPE
100:0
80:20
60:40
50:50
40:60
20:80
0:100

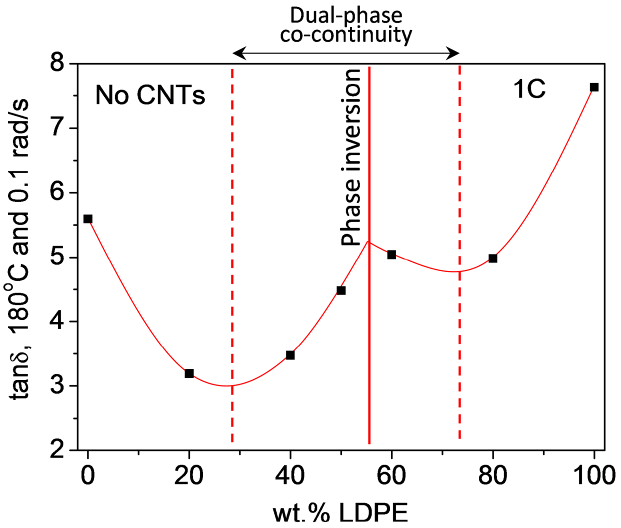
Dual-phase co-continuity
No CNTs
Phase inversion
1C
tanδ, 180°C and 0.1 rad/s
wt.% LDPE
2
3
4
5
6
7
8
0
20
40
60
80
100

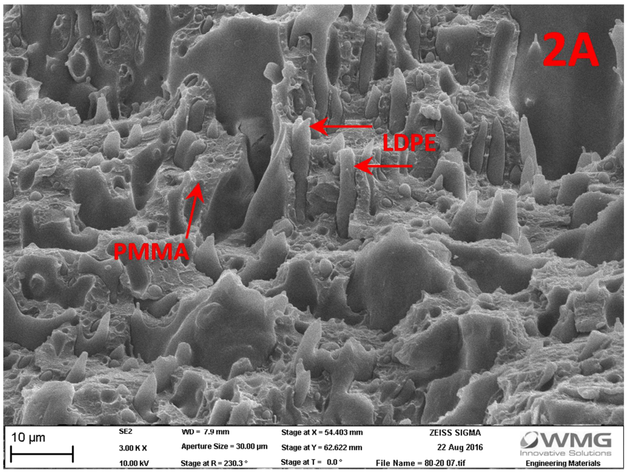
2A
LDPE
PMMA
10 µm
SE2
3.00 K X
10.00 kV
WD = 7.9 mm
Aperture Size = 30.00 µm
Stage at R = 230.3 °
Stage at X = 54.403 mm
Stage at Y = 62.622 mm
Stage at T = 0.0 °
ZEISS SIGMA
22 Aug 2016
File Name = 80-20 07.tif
WMG
Innovative Solutions
Engineering Materials

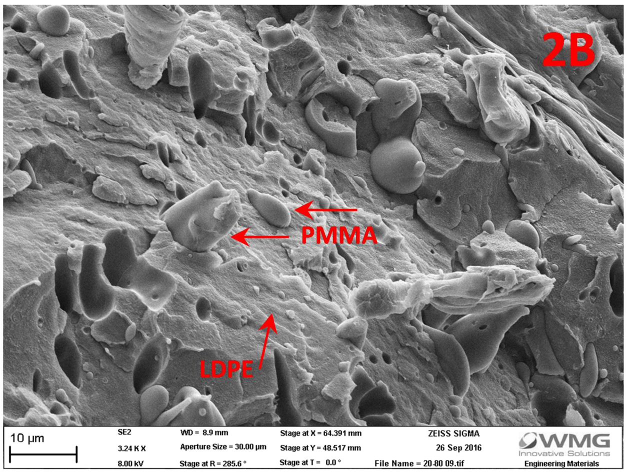
2B
PMMA
LDPE
10 µm
SE2
3.24 K X
8.00 kV
WD = 8.9 mm
Aperture Size = 30.00 µm
Stage at R = 285.6 °
Stage at X = 64.391 mm
Stage at Y = 48.517 mm
Stage at T = 0.0 °
ZEISS SIGMA
26 Sep 2016
File Name = 20-80 09.tif
WMG
Innovative Solutions
Engineering Materials

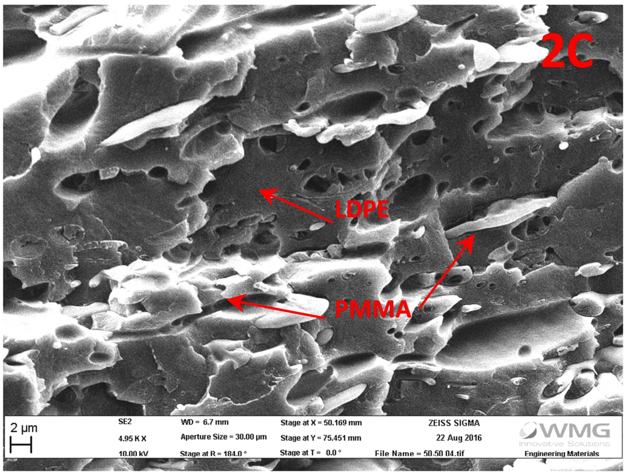
2C
LDPE
PMMA
2 µm
SE2
4.95 K X
10.00 kV
WD = 6.7 mm
Aperture Size = 30.00 µm
Stage at R = 184.0 °
Stage at X = 50.169 mm
Stage at Y = 75.451 mm
Stage at T = 0.0 °
ZEISS SIGMA
22 Aug 2016
File Name = 50-50 04.tif
WMG
Innovative Solutions
Engineering Materials

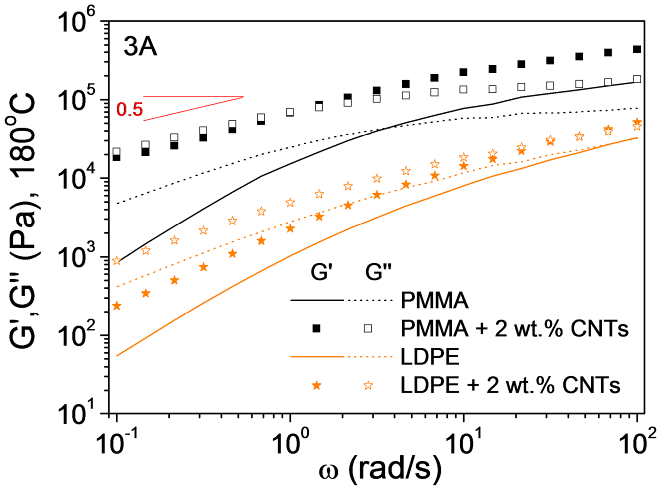
3A
0.5
G',G'' (Pa), 180°C
ω (rad/s)
G' G''
PMMA
PMMA + 2 wt.% CNTs
LDPE
LDPE + 2 wt.% CNTs
10^1
10^2
10^3
10^4
10^5
10^6
10^{-1}
10^0
10^1
10^2

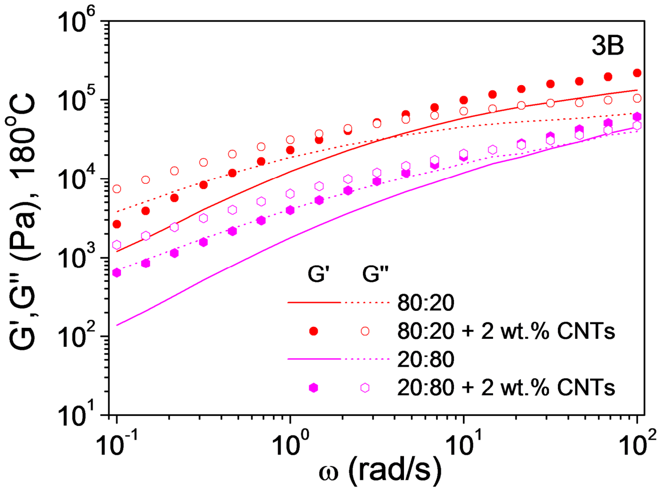
3B
G',G'' (Pa), 180°C
ω (rad/s)
G' G''
80:20
80:20 + 2 wt.% CNTs
20:80
20:80 + 2 wt.% CNTs
10^1
10^2
10^3
10^4
10^5
10^6
10^{-1}
10^0
10^1
10^2

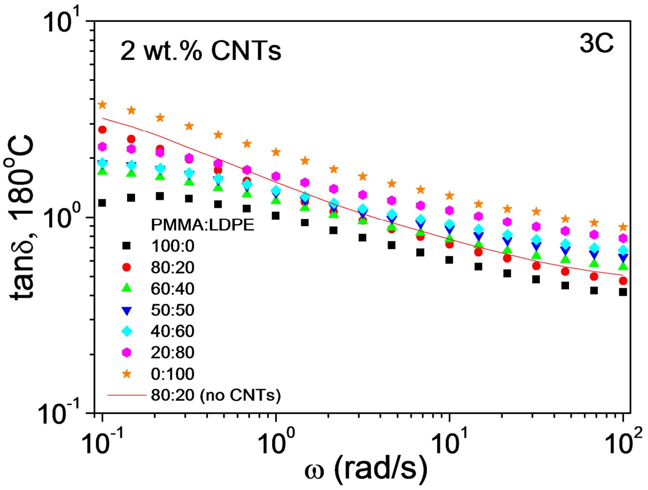
2 wt.% CNTs
3C
tanδ, 180°C
ω (rad/s)
PMMA:LDPE
100:0
80:20
60:40
50:50
40:60
20:80
0:100
80:20 (no CNTs)
10^{-1}
10^0
10^1
10^{-1}
10^0
10^1
10^2

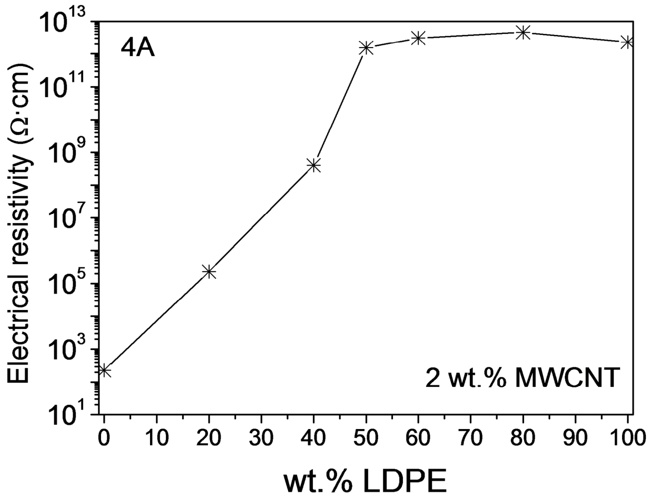
4A
2 wt.% MWCNT
Electrical resistivity (Ω·cm)
10^{13}
10^{11}
10^{9}
10^{7}
10^{5}
10^{3}
10^{1}
0
10
20
30
40
50
60
70
80
90
100
wt.% LDPE

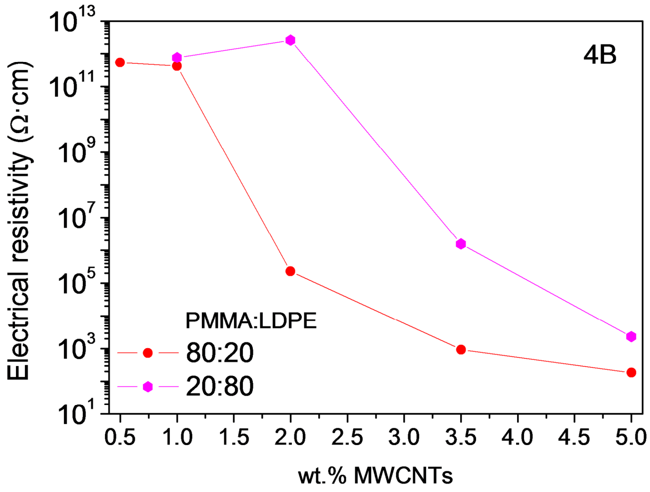
4B
PMMA:LDPE
80:20
20:80
Electrical resistivity (Ω·cm)
10^{13}
10^{11}
10^{9}
10^{7}
10^{5}
10^{3}
10^{1}
0.5
1.0
1.5
2.0
2.5
3.0
3.5
4.0
4.5
5.0
wt.% MWCNTs

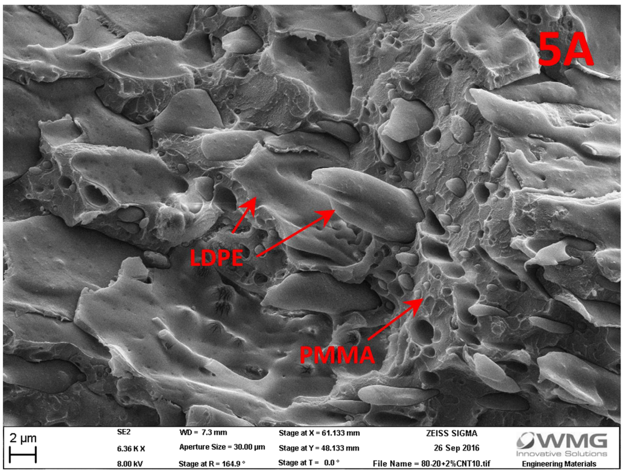
5A
LDPE
PMMA
2 µm
SE2
6.36 K X
8.00 kV
WD = 7.3 mm
Aperture Size = 30.00 µm
Stage at R = 164.9 °
Stage at X = 61.133 mm
Stage at Y = 48.133 mm
Stage at T = 0.0 °
ZEISS SIGMA
26 Sep 2016
File Name = 80-20+2%CNT10.tif
WMG
Innovative Solutions
Engineering Materials

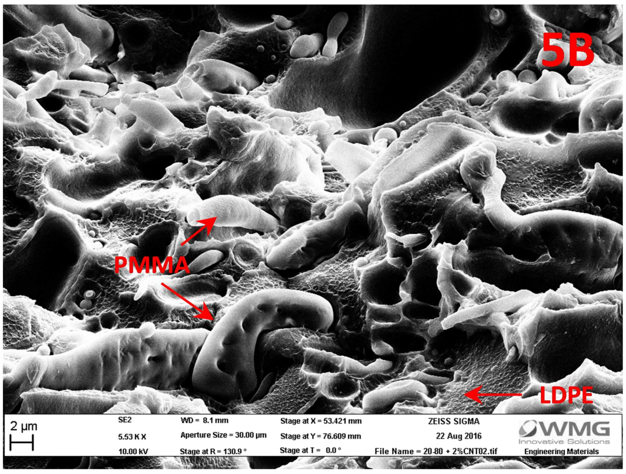
5B
PMMA
LDPE
2 µm
SE2
5.53 K X
10.00 kV
WD = 8.1 mm
Aperture Size = 30.00 µm
Stage at R = 130.9 °
Stage at X = 53.421 mm
Stage at Y = 76.609 mm
Stage at T = 0.0 °
ZEISS SIGMA
22 Aug 2016
File Name = 20-80 + 2%CNT02.tif
WMG
Innovative Solutions
Engineering Materials

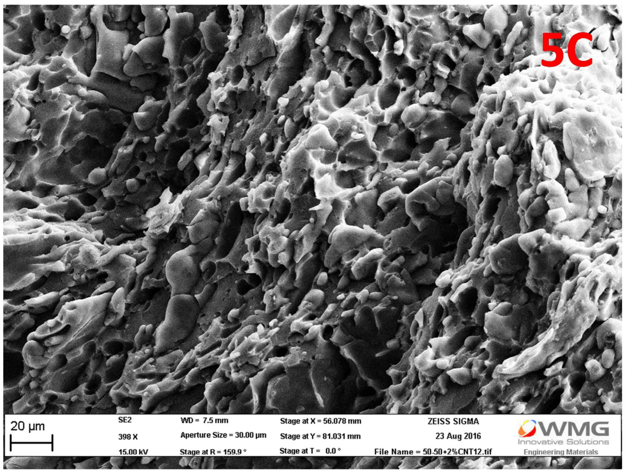
5C
20 µm
SE2
398 X
15.00 kV
WD = 7.5 mm
Aperture Size = 30.00 µm
Stage at R = 159.9 °
Stage at X = 56.078 mm
Stage at Y = 81.031 mm
Stage at T = 0.0 °
ZEISS SIGMA
23 Aug 2016
File Name = 50-50+2%CNT12.tif
WMG
Innovative Solutions
Engineering Materials

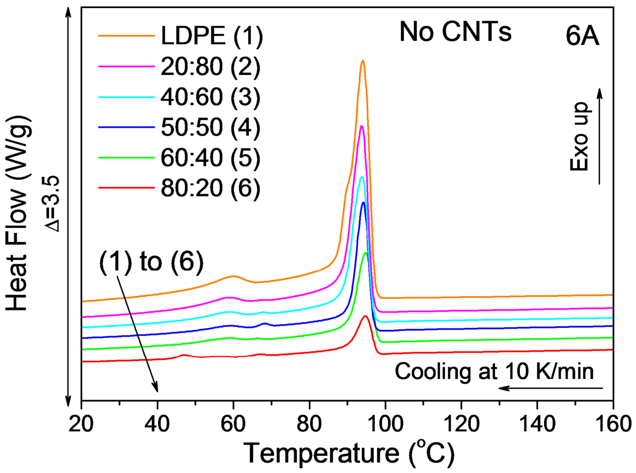
LDPE (1)
20:80 (2)
40:60 (3)
50:50 (4)
60:40 (5)
80:20 (6)
No CNTs
6A
Exo up
(1) to (6)
Cooling at 10 K/min
Heat Flow (W/g)
Δ=3.5
20
40
60
80
100
120
140
160
Temperature (°C)

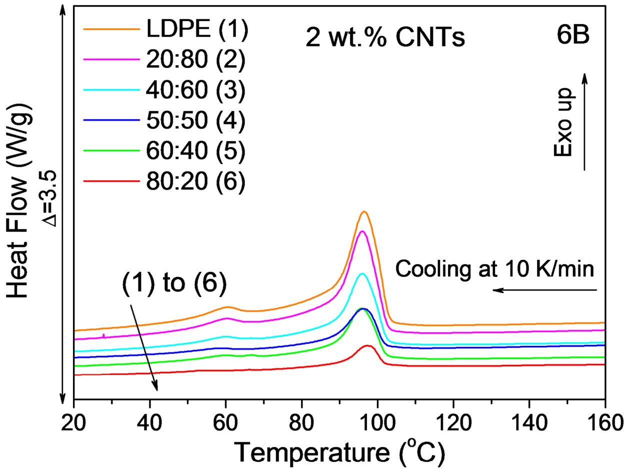
LDPE (1)
20:80 (2)
40:60 (3)
50:50 (4)
60:40 (5)
80:20 (6)
2 wt.% CNTs
6B
Exo up
Cooling at 10 K/min
(1) to (6)
Heat Flow (W/g)
Δ=3.5
20
40
60
80
100
120
140
160
Temperature (°C)

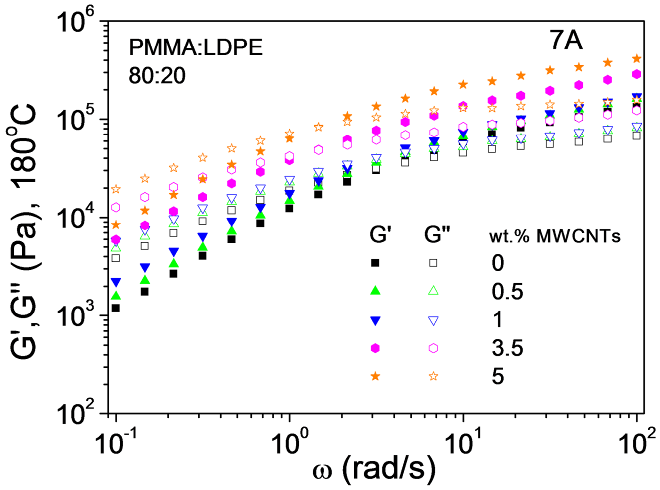
7A
PMMA:LDPE
80:20
G',G'' (Pa), 180°C
ω (rad/s)
10^2
10^3
10^4
10^5
10^6
10^-1
10^0
10^1
10^2
G'
G''
wt.% MWCNTs
0
0.5
1
3.5
5

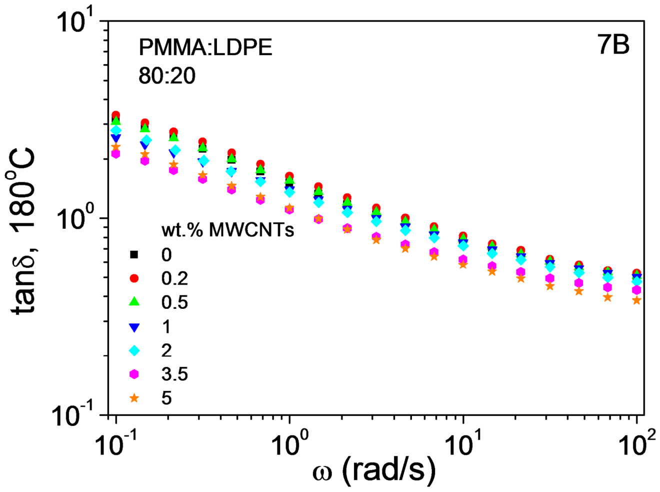
7B
PMMA:LDPE
80:20
tanδ, 180°C
ω (rad/s)
10^-1
10^0
10^1
10^-1
10^0
10^1
10^2
wt.% MWCNTs
0
0.2
0.5
1
2
3.5
5

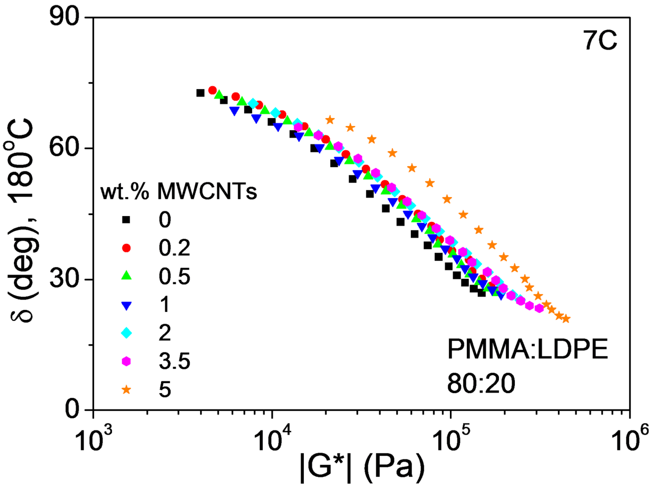
7C
PMMA:LDPE
80:20
δ (deg), 180°C
|G*| (Pa)
0
30
60
90
10^3
10^4
10^5
10^6
wt.% MWCNTs
0
0.2
0.5
1
2
3.5
5

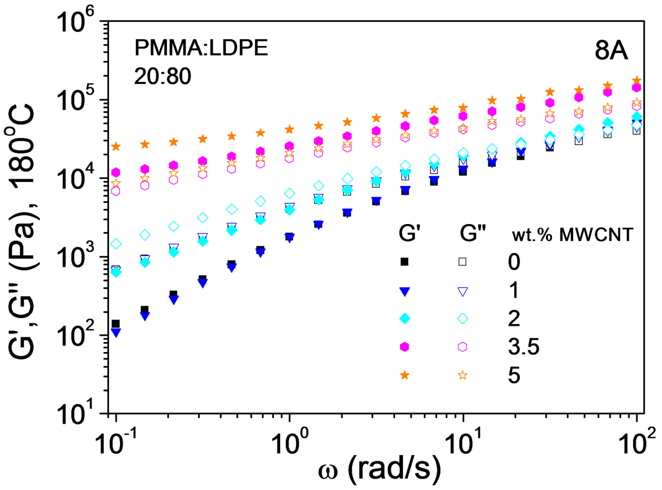
PMMA:LDPE
20:80
8A
G',G'' (Pa), 180°C
ω (rad/s)
10^1
10^2
10^3
10^4
10^5
10^6
10^-1
10^0
10^1
10^2
G'
G''
wt.% MWCNT
0
1
2
3.5
5

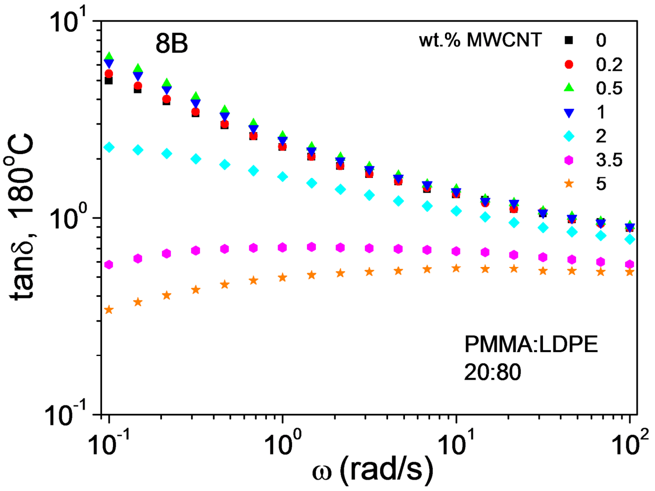
8B
wt.% MWCNT
0
0.2
0.5
1
2
3.5
5
PMMA:LDPE
20:80
tanδ, 180°C
ω (rad/s)
10^-1
10^0
10^1
10^-1
10^0
10^1
10^2

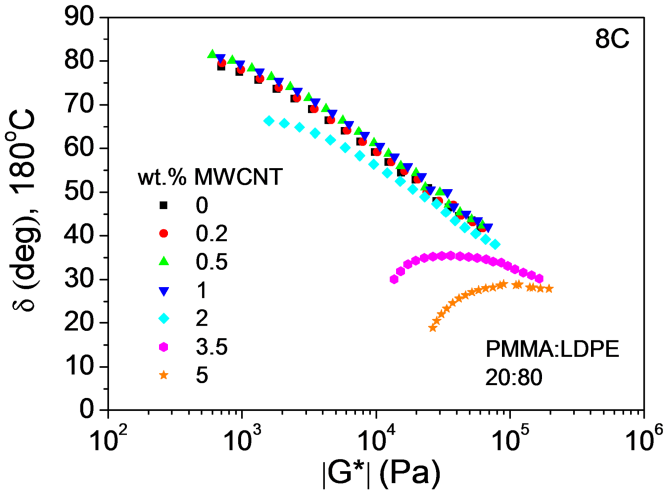
8C
δ (deg), 180°C
|G*| (Pa)
0
10
20
30
40
50
60
70
80
90
10^2
10^3
10^4
10^5
10^6
wt.% MWCNT
0
0.2
0.5
1
2
3.5
5
PMMA:LDPE
20:80

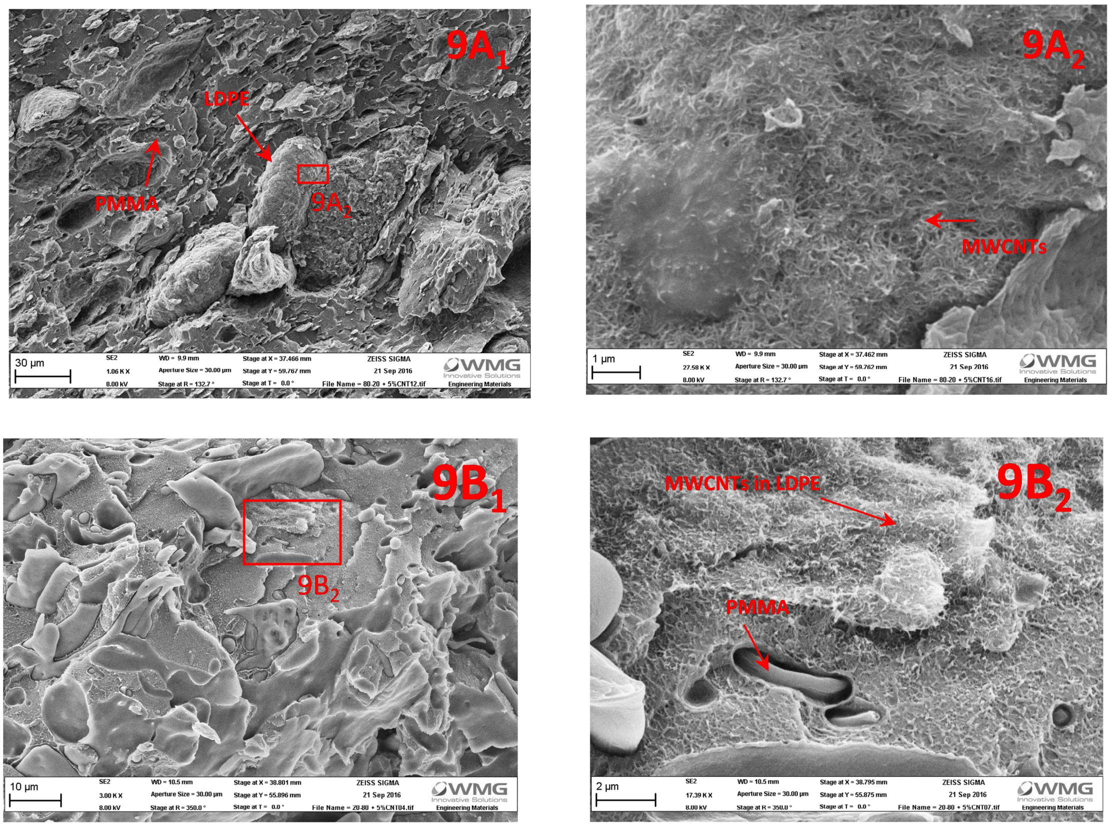
9A$_1$
LDPE
PMMA
9A$_2$
30 µm
9A$_2$
MWCNTs
1 µm
9B$_1$
9B$_2$
10 µm
9B$_2$
MWCNTs in LDPE
PMMA
2 µm

On the phase affinity of multi-walled carbon nanotubes in PMMA:LDPE immiscible polymer blends

Claudia Roman, Moisés García-Morales[*], Jaipal Gupta and Tony McNally

HIGHLIGHTS:

- MWCNTs located in the thermodynamically less favorable LDPE phase
- MWCNT localization governed by polymer phase first to melt
- Electrical conductivity determined by double percolation
- Bulk linear viscoelasticity controlled by the major polymer phase